THE JOURNAL OF PHYSICAL CHEMISTRY B

Article

pubs.acs.org/JPCB

How the Type of Cosurfactant Impacts Strongly on the Size and Interfacial Composition in Gemini 12-2-12 RMs Explored by DLS, SLS, and FTIR Techniques

Victor E. Cuenca, R. Darío Falcone, Juana J. Silber, and N. Mariano Correa*

Departamento de Química, Universidad Nacional de Río Cuarto, Agencia Postal # 3. C.P., X5804BYA Río Cuarto, Argentina

Supporting Information

ABSTRACT: The limited amount of information about reverse micelles (RMs) made with gemini surfactants, the effect of the *n*-alcohols in their interface, and the water-entrapped structure in the polar core motivated us to perform this work. Thus, in the present contribution, we use dynamic light scattering (DLS), static light scattering (SLS), and FT-IR techniques to obtain information on RMs structure created, with the gemini dimethylene-1,2-bis-(dodecyldimethylammonium) bromide (G12-2-12) surfactant and compare the results with its monomer: dodecyltrimethylammonium bromide (DTAB). In this way, the size of the aggregates formed in different nonpolar organic solvents, the effect of the chain length of *n*-alcohols used as cosurfactants, and the water-entrapped structure were explored. The data show that the structure of the cosurfactant needed to stabilize the RMs plays a fundamental role, affecting the size and behavior of the aggregates. In contrast to what happens with the RMs formed with the monomer DTAB, water entrapped inside G12-2-12 RMs displays different interaction with the interface depending on the hydrocarbon chain length of the *n*-alcohol used as cosurfactant. Thus, *n*-pentanol and *n*-octanol molecules are located in different regions in the RMs interfaces formed with the gemini surfactant. *n*-Octanol locates at the RMs interface among the surfactant hydrocarbon tails increasing the water−surfactant polar headgroup interaction. On the other hand, *n*-pentanol locates at the RMs interface near the polar core, limiting the interaction of water with the micellar inner interface and favoring the water−water interaction in the polar core.

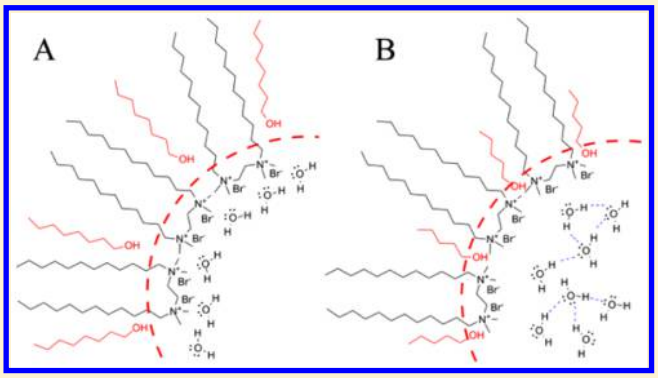

1. INTRODUCTION

Reverse micelles (RMs) have attracted considerable attention in the past two decades due to their ability to host hydrophilic components in organic solvents[1,2] and, at the present, for the ability to act as scaffold in the synthesis of nanostructures.[3,4] RMs are aggregates of surfactants dispersed in a nonpolar solvent, in which the polar head groups of the surfactants point inward and the hydrocarbon chains point toward to the nonpolar pseudophase. Thus, water is easily solubilized in the polar core, and the amount dispersed can be quantified as the molar ratio W_0 (W_0 = [Water]/[Surfactant]). The structure of the water solubilized inside the RMs depends on the type of surfactant used and W_0 among others, and in many cases, the structures may display unique properties.[5,6]

It is known that cationic surfactants, such as cetyltrimethylammonium bromide (CTAB), need the addition of cosurfactant in order to form stable RMs.[7,8] Although the addition of *n*-alcohols of different chain length as cosurfactants results in a strong modification of the micelle interface, there are scarce efforts to elucidate the effect that the alcohol has on different interfacial properties.[9] Short *n*-alcohol molecules tend to locate in the polar part of the interface interacting with the polar head of the surfactants, reducing the repulsion between the polar moieties of the surfactants. On the contrary, those molecules with long hydrocarbon chain tend to locate in the outer part, the nonpolar environment, of the RMs, thereby enhancing the interaction of the surfactant tails and reducing the interactions between RMs droplets.[10−13] This particular behavior of surfactants with *n*-alcohols affects greatly the amount of water that the cationic RMs are able to encapsulate.[14] Many studies on the properties of RMs (droplet size, micropolarity, critical micelle concentration (CMC)) have been conducted using "monomeric" surfactants (CTAB,[7] benzyl-*n*-hexadecyldimethylammonium chloride (BHDC),[15] tetradecyltrimethylammonium bromide (TTAB),[16] didodecyldimethylammonium chloride (DDAC),[17] etc.), but there have been few reports using gemini surfactants to form RMs.[18,19] Gemini surfactants are made up of two amphiphilic moieties linked, at their polar head level by a spacer.[19,20] Quaternary ammonium gemini surfactants have a nomenclature of the type *m-s-m* where *m* indicates the number of carbons atoms in the hydrophobic chain, and *s* indicates those in the spacer.

Received: October 22, 2015
Revised: December 30, 2015
Published: January 5, 2016

DOI: 10.1021/acs.jpcb.5b10380
J. Phys. Chem. B 2016, 120, 467−476

Solubilized in water, gemini surfactants have gathered some attention because of their extraordinary properties like small CMC values in comparison with their monomers, excellent wetting and foaming abilities,[21] great variety of micellar shape,[22,23] and rheological properties.[24] However, studies on their properties in RM systems are scarce.[18,25] CMC values of the system G12-s-12/*n*-hexanol/*n*-heptane varying *s* revealed a dependence with the length of the spacer *s*, increasing with *s* from *s* = 2 to *s* = 5 and then CMC decreases with *s*.[26] Studies of the water structure dispersed by RMs were done through FT-IR experiments revealing the presence of four different water types inside the RMs: bulk-like water, cation-bound water, anion-bound water and free water, which structures depend on the W_0 value.[27] However, these experiments are open to discussion because they do not take into account the possibility of the overlapping of the O−H overtones in the vibrational band when pure water is used as were noted by Novaki et al.[28] The limited amount of information about RM media made with gemini surfactants, the effect of the *n*-alcohols on interfacial properties, and the water entrapped structure in the polar core opens an interesting field of investigation. Thus, in the present work, we study RMs formed with the gemini surfactant: dimethylene-1,2-bis(dodecyldimethylammonium) bromide (G12-2-12, see structure in Scheme 1A) in benzene using

Scheme 1. Chemical Structures of G12-2-12 (A) and DTAB (B) Surfactants

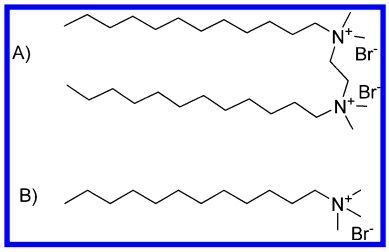

Dynamic Light Scattering (DLS), Static Light Scattering (SLS) and FT-IR techniques to obtain information on different RMs properties. In this way, the size of the aggregates, the effect of the chain length of the cosurfactants, and the water-entrapped structure were explored. Also, the results for RMs made with the monomer dodecyltrimethylammonium bromide (DTAB, Scheme 1B) surfactant are shown for comparison.

2. EXPERIMENTAL SECTION

2.1. Materials. *N,N,N′,N′*-Tetramethylethylenediamine (electrochemical purity 99,5%) was purchased from Aldrich and used without further purification. Dodecyl bromide was purchased from Merck and purified using activated carbon which was later removed by filtration. Dodecyltrimethylammonium bromide (DTAB, Aldrich, 98%) was recrystallized twice from ethanol (Cicarelli, 99.5%) and dried under vacuum prior to use. Milli-Q water (18.2 MΩ.cm) was used as polar solvent in the preparation of RMs solutions. D_2O and benzene from Sigma (HPLC quality) were used without prior purification. Monodeuterated water (HOD) was prepared by stirring a solution of 10% D_2O in H_2O at room temperature for 1 h in order to allow the exchange of H and D. Except those otherwise noted, all solvents employed were HPLC grade and were used without further purification. Synthesis and characterization of the Gemini 12-2-12 Surfactant (G12-2-12) is detailed in the Supporting Information.

2.2. Methods. *2.2.1. RMs Preparation.* Volumetric dilution method was used to prepare the *n*-alcohols:benzene stocks solutions. Stock solutions of the surfactant (G12-2-12 or DTAB) and/or water/surfactant were prepared by weight. In order to prepare the solutions with variable W_0, stock solutions were pipetted in 2 mL volumetric flasks, and the adequate amount of water was incorporated into each micellar solutions using calibrated microsyringes. Benzene saturated with monodeuterated water was prepared by adding 20 μL of 10% monodeuterated water to 2 mL of benzene; this mixture was stirred for 24 h and then allowed to rest for a day. It should be noted that to prepare gemini systems at the highest surfactant concentration, 0.1 M, the RMs require the addition of a minimum amount of water (W_0^{min}) to dissolve the surfactant and to form a clear isotropic solution for both cosurfactant used: *n*-pentanol and *n*-octanol (Table 1).

Table 1. Maximum Amount of Water Solubilized (W_0^{max}) in Benzene/G12-2-12/*n*-Alcohol and Benzene/DTAB/*n*-Alcohol Systems at Two [surfactant] = 0.1 and 0.01 M [*n*-alcohol] = 0.7 M and *T* = 25 °C

system	[surfactant] (M)	W_0^{max}
benzene/G12-2-12/*n*-octanol[a]	0.1	28
benzene/G12-2-12/*n*-octanol	0.01	31
benzene/DTAB/*n*-octanol	0.1	20
benzene/DTAB/*n*-octanol	0.01	22
benzene/G12-2-12/*n*-pentanol[b]	0.1	41
benzene/G12-2-12/*n*-pentanol	0.01	40
benzene/DTAB/*n*-pentanol	0.1	23
benzene/DTAB/*n*-pentanol	0.01	27

[a]The systems require a minimum amount of water to solubilize the surfactant. W_0^{min} = 4.6. [b]W_0^{min} = 5.0.

2.2.2. FT-IR Experiments. FT-IR spectra were recorded with a Nicolet IMPACT 400 spectrometer. The FT-IR measurements for the RMs samples were taken in Irtran-2 cell of 0.5 mm path length from Wilmad Glass (Buena, NJ). FT-IR spectra were obtained by coadding 200 spectra at a resolution of 0.5 cm^{-1}. The monodeuterated water solutions (10% D_2O in water) were prepared by volumetric dilution. The reason for using partially deuterated water is explained in the Discussion Section. The spectral band of HOD is superimposed on a finite background which could be approximated with the spectrum of pure water.[29−32] Therefore, the reference sample, at each W_0 value, was a surfactant solution containing matched [water]/[surfactant]. Deconvolution of the HOD spectral band was carried out by Microcal OriginPro 9.0 SR2 using a Voigt function.

2.2.3. DLS Experiments. The diameters of the RMs were determined by DLS (Malvern 4700 with goniometer and correlator) with an argon-ion laser operating at 488 nm. Samples were filtered using an Acrodisc with 0.2 μm PTFE membrane (Sigma). Viscosities and refractive indices of the solvent mixtures are required for the DLS analyses: the viscosities of benzene, *n*-pentanol, and *n*-octanol were taken from the literature.[33] The refractive indices of the solvent mixtures were calculated using a first-order approximation (eq 1).

$$\eta_D = X_1\eta_{D1} + X_2\eta_{D2} \quad (1)$$

where η_{D1} and η_{D2} are the pure solvent refractive indices. The effect of temperature on η_D of these solvents was found to be

DOI: 10.1021/acs.jpcb.5b10380
J. Phys. Chem. B 2016, 120, 467−476

sufficiently small to be ignored. Multiple samples for each size were made, and 30 independent size measurements were made for each individual sample. All the measurements were carried out using quartz fluorescence cell at a scattering angle of 90° at a temperature of 25.0 ± 0.1 ∘C. The DLS experiments were analyzed using CONTIN algorithm.

2.2.4. SLS Measurements. The SLS technique was used to determine the micellar molecular weights. Due to the small size of the RMs droplets, the data analysis of SLS was done using the Rayleigh expression[34] shown in eq 2:

$$\frac{KC}{R_\theta} = \frac{1}{M_w} + 2A_2C \tag{2}$$

where C is the surfactant concentration, R_θ is the Rayleigh ratio of the sample intensity to the incident intensity at the angle θ, M_w is the molecular weight of the sample in weight-average, A_2 is the second virial coefficient and K is an optical constant that accounts for the experimental parameters:

$$K = \frac{4\pi^2 n_0^2}{\lambda_0^4 N_a}\left(\frac{dn}{dC}\right)^2 \tag{3}$$

where dn/dC is the increment in the refractive index with concentration, n_0 is the solvent refractive index, λ_0 is the wavelength of the incident light, and N_a is the Avogadro number. Calibration was performed using toluene, for which the reported Rayleigh ratio[35] at 90° and at a wavelength of 488 nm (R_{90}^{tol}) is 3.96×10^{-5} cm^{-1}. Linear increment in refractive index with concentration (dn/dC) was measured using a differential refractometer (BI-DNDC Brookhaven Instruments Corporation) at a fixed wavelength of 470 nm and 25 °C in a surfactant concentration range from 1×10^{-3} M to 0.1 M.

The value of the excess Rayleigh ratio at an angle of 90°, R_{90}, has been obtained with reference to the known Rayleigh ratio of toluene.

$$R_{90} = S_{90} * R_{90}^{tol} \tag{4}$$

where $S_{90} = (I_S - I_W)/I_{tol}$ is the normalized intensity of the sample with respect to the standard, in which I_S is the value of the intensity of light scattered at 90°, I_W the intensity of light scattered by a cell containing pure solvent, and I_{tol} the light scattered of the toluene. S_{90} was obtained at several surfactant concentrations measured at 25 °C.

2.2.5. Dilution Method. When a fixed amount of water, nonpolar solvent, surfactant, and cosurfactant form a stable water in oil (W/O) microemulsion, the distribution of a cosurfactant between the interfacial region consisting of surfactant molecules and the external nonpolar phase is guided by an appropriate distribution constant that depends, among other parameters, on the equilibrium temperature of the system. Increasing the nonpolar solvent content alters the interfacial concentration of the cosurfactant and consequently makes the system unstable. This can be compensated by adding a small amount of cosurfactant sufficient to regain the interfacial concentration necessary for a stable dispersion and, thus, reestablishing the distribution constant. This is the process followed in a dilution experiment proposed by Birdi[36] and Singh et al.,[37] and subsequent analytical treatment using equilibrium thermodynamics was proved correct by Moulik et al.[38]

The expression used for the data analysis of the dilution experiments is obtained as follows. Supposing the number of moles of *n*-alcohol at the interface, in bulk nonpolar phase and in the water pool are n^i_a, n^o_a and n^w_a respectively, the total number of moles of *n*-alcohol n_a is defined in eq 5:

$$n_a = n^i_a + n^o_a + n^w_a \tag{5}$$

where the number of moles of *n*-alcohol in water, n^w_a, are negligible because of its very small solubility. If n_s and n_o are the total number of moles of surfactant and benzene, and if $a = (n^i_a)/n_s$ and $b = (n^o_a)/n_o$, then the molar fraction values of the *n*-alcohol in the interface (X^i_a) and in the oil phase (X^o_a) can be calculated as follows

$$X^i_a = \frac{n^i_a}{n^i_a + n_s} = \frac{n^i_a/n_s}{n^i_a/n_s + 1} = \frac{a}{a+1} \tag{6}$$

$$X^o_a = \frac{n^o_a}{n^o_a + n_o} = \frac{n^o_a/n_o}{n^o_a/n_o + 1} = \frac{b}{b+1} \tag{7}$$

Using eq 6 and 7, eq 5 can be rewritten as eq 8

$$\frac{n_a}{n_s} = a + b\left(\frac{n_o}{n_s}\right) \tag{8}$$

In the dilution experiment at fixed n_s, the values of n_a and n_o are varied so it is possible to obtain a series of n_a/n_s and n_o/n_s values, whose graphical plots according to eq 8 yield the values of a and b from the intercept and the slope, respectively.

The distribution constant for the *n*-alcohol between the micellar interface and the oil phase, K_d, can be obtained from eq 9:

$$K_d = \frac{X^i_a}{X^0_a} = \frac{a(b+1)}{b(a+1)} \tag{9}$$

Rearranging eq 6, eq 10 is obtained.

$$n^i_a = \frac{X^i_a}{1 - X^i_a} * n^i_s \tag{10}$$

2.2.6. Micellar Composition. The aggregation number, N_{agg}, is a very important parameter in the characterization of a micellar system. In a system containing two components, nonpolar solvent and surfactant molecules (binary systems), the procedure to obtain this parameter is fairly simple, requiring only the surfactant molecular weight and the micellar weight-average molecular weight (M_w). However, in a system containing four components (quaternary systems) as ours, the determination of the surfactant aggregation number is not straightforward. Thus, for a system composed by a nonpolar external solvent, surfactant, cosurfactant, and polar solvent located inside the RMs the micellar M_w can be expressed as the sum of its constitutive components as eq 11 shows:

$$M_w = M_{water} * W_0 * n^i_s + M_{surfactant} * n^i_s + M_{alcohol} * n^i_a \tag{11}$$

where M_{water}, $M_{surfactant}$, and $M_{alcohol}$ are the molecular weight of water, G12-2-12 surfactant and cosurfactant, respectively, n^i_s and n^i_a are the moles of surfactant and cosurfactant molecules at the micellar interface, respectively.

Introducing eq 10 in eq 11 and with rearrangement, eq 12 is obtained:

$$n^i_s = \frac{M_w}{M_{water} * W_0 + M_{surfactant} + M_{alcohol} * \frac{X^i_a}{1 - X^i_a}} \tag{12}$$

DOI: 10.1021/acs.jpcb.5b10380
J. Phys. Chem. B 2016, 120, 467−476

From which the number of surfactant molecules at the interface ($n^{i}_{s} = N_{agg}$) can be calculated.

3. RESULTS AND DISCUSSION

3.1. Solubilization of G12-2-12 in the Nonpolar Solvents. In order to evaluate if the surfactant G12-2-12 can be used to generate RMs, the first experiment performed was to explore the phase diagram of the ternary system keeping constant the surfactant concentration and changing the amount of water dispersed. First, G12-2-12 solubility in different nonpolar solvents such as *n*-heptane, chlorobenzene and benzene was tested. The solubility of the surfactant was very low (less than 1×10^{-3} M) in all nonpolar solvents tested, but the solubility in aromatic solvents was highly enhanced by the addition of *n*-alcohols. Two *n*-alcohols were selected, *n*-pentanol and *n*-octanol, in order to evaluate if the length of the hydrocarbon chain of the *n*-alcohol affects the amount of water that the system dissolves. The amount of *n*-alcohol required to form an isotropic solution was 0.7 M for every experiment, concentration which allowed us to work in an adequate range of surfactant concentration yielding stable solutions.

3.2. Solubilization of Water in Benzene/G12-2-12 Systems. The systems formed by benzene/G12-2-12/*n*-pentanol/water and benzene/G12-2-12/*n*-octanol/water were evaluated to determine the amount of water that both systems can solubilize forming clear and stable quaternary mixtures. In Table 1 is summarized the maximum amount of water solubilized (W_0^{max}) in benzene/G12-2-12/*n*-alcohol and benzene/DTAB/*n*-alcohol systems at two [surfactant] = 0.1 and 0.01 M. It should be noted that W_0 values are defined using the total surfactant concentration for DTAB and G12-2-12.

The results show that G12-2-12 solutions with *n*-pentanol as cosurfactant accept larger amount of water in comparison with those formed with *n*-octanol. Moreover, changes in the gemini concentration do not affect the W_0^{max} values. The explanation for this will be demonstrated in the next section. Herein, we will highlight that the reasons are the different water structure and water−surfactant interaction inside both RMs. When *n*-pentanol is used as cosurfactant it interacts strongly with the polar head of the gemini surfactant, and water interacts strongly with other water molecules with the consequent increases in the water content.

Interestingly, if we compare the RMs formed with the gemini surfactant with the one formed with the monomer, it can be seen that RMs formed with G12-2-12 surfactant and *n*-pentanol as cosurfactant show a 2-fold increase in the amount of water accepted in comparison with the systems formed with DTAB. For *n*-octanol as cosurfactant, the situation is different because both RMs accept the same total amount of water. Considering that the gemini surfactant has two polar heads per mole (Scheme 1A), it can be deduced that the monomer accepts more water per polar headgroup than the gemini surfactant. These results also suggest that the different location of the *n*-alcohols at the RMs interface is the explanation for this result. *n*-Octanol is located in the oil side of the interface (as we will demonstrate in the next section), and water interacts with the polar head of the surfactant increasing the droplet size and probably the droplet−droplet interaction.

3.3. RMs Formation Studied by DLS Technique. Considering the complexity of the quaternary systems under study, the question to be answered is if the water molecules added are effectively encapsulated by the surfactant creating a true RMs or if water molecules are dissolved only in the benzene/G12-2-12/*n*-alcohol mixtures without any molecular organization (bicontinuous microemulsion)?[1,39] Other question is whether molecules located at the interface are in the nonpolar pseudophase or in the water domain? In this work, DLS was used to assess this matter for benzene/G12-2-12/*n*-alcohol systems. Thus, if water is really encapsulated forming RMs, the droplet sizes must increase when the W_0 value increases with a linear tendency (swelling law of RMs) as it is well-established for water or polar solvents/surfactant RMs systems.[40] This feature also demonstrates that the RMs consist of discrete spherical and noninteracting droplets.[41] On the other hand, if the polar solvent is not encapsulated by the surfactant, the droplet sizes remain constant or even decrease with the polar solvent addition.[39] To the best of our knowledge, the droplet sizes of G12-2-12 in benzene system have never been reported.

It is known that the RMs droplet sizes depend, among many other variables, on the effective packing parameter of the surfactants, v/al_c, in which v and l_c are the volume and the length of the hydrocarbon chain, respectively, and a is the surfactant headgroup area. The RMs sizes are larger when the surfactant packing parameter values are smaller. In this sense, we have previously demonstrated[42] that polar solvents that strongly interact with the RM interface lead to an increase in the effective surfactant headgroup area a. Moreover, it was also demonstrated that the RMs droplet sizes depend strongly on the kind of interactions that the different polar solvents can make with the surfactant rather than their molar volume even when a solvent mixture is confined at a nanoscale size.[12,42] On the other hand, if the interaction between the polar solvent and the interface is small, the droplet size values seem to depend slightly on the polar solvent content.[39,42,43]

All the DLS experiments were carried out at fixed surfactant concentration (0.1 M) and the RMs solutions are not at infinite dilution. Hence, it is appropriate to introduce an apparent hydrodynamic diameter (d_{app}) in order to make the comparison with the system herein studied as it was used before.[44]

Figure 1 represents the d_{app} values of the RMs obtained by DLS at different W_0 for all the systems studied. Additionally, in Table S1 (Supporting Information) are reported the polydispersity index (PDI) values obtained. From the data shown in Figure 1, it can be seen that different profiles are obtained for G12-2-12 RMs than DTAB systems, especially at $W_0 < 10$. Additionally, for the gemini surfactant an unusual dependence of the *n*-alcohol used is observed. Thus, the systems containing benzene/DTAB/*n*-pentanol/water and benzene/DTAB/*n*-octanol/water exhibit a linear dependence of the hydrodynamic diameter with the W_0 in the whole range investigated, indicating that the water is being encapsulated inside the RMs and that the system is formed by discrete spherical aggregates.[45]

For the benzene/G12-2-12/*n*-octanol/water system, a linear trend of the d_{app} values with the increase of W_0 value is also found. However, at low water content, the droplet size values are quite different in comparison with benzene/DTAB/*n*-octanol/water RMs. For example, at $W_0 = 5$ in benzene/G12-2-12/*n*-octanol/water d_{app} is 5.5 nm but 3 nm for benzene/DTAB/*n*-octanol/water. When the W_0 is larger, the droplets sizes are similar for both RMs. These facts suggest that the gemini surfactant chemical structure greatly affects its packing parameter when the hydration level is low. The distance between the polar heads of surfactants in a micelle is called

DOI: 10.1021/acs.jpcb.5b10380
J. Phys. Chem. B 2016, 120, 467−476

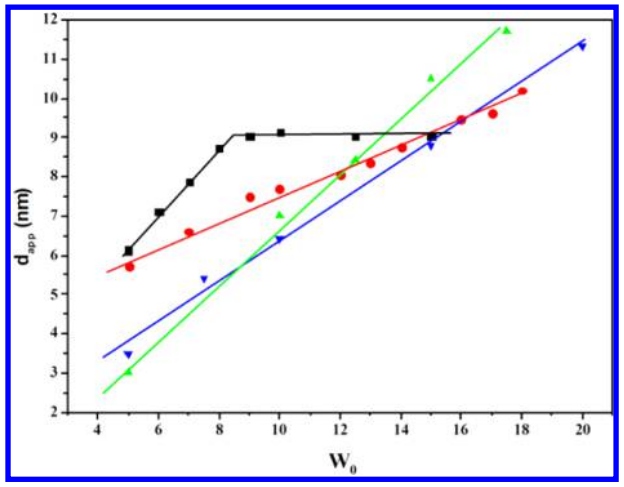

Figure 1. Apparent hydrodynamic diameter (d_{app}) of all the RMs studied as a function of W_0 obtained by DLS technique. Benzene/G12-2-12/*n*-pentanol/water (■); benzene/G12-2-12/*n*-octanol/water (red ●); benzene/DTAB/*n*-pentanol/water (green ▲); benzene/DTAB/*n*-octanol/water (blue ▼). [Surfactant] = 0.1 M, [*n*-alcohol] = 0.7 M, T = 25 ± 0.1 °C. The lines are drawn to guide the eye.

distribution of distances, and it displays a maximum at a thermodynamic equilibrium distance determined by the opposite forces at play in micelle formation (dispersive forces, electrostatic interactions, entropy, etc.).[46] In the early works of Danino et al.,[47] it was proposed that distribution of distances between polar head groups of gemini surfactants forming direct micelles would be bimodal. This idea was later confirmed by computer simulation indicating that polar head groups within gemini surfactants with short spacers are subject to great repulsion energy as they are closer that thermodynamic equilibrium would require.[48] In the RMs formation, two positively charged headgroups linked by a short spacer would require great solvation in order to closely pack into a RM, and thus, the effective area of the surfactant would increase, leading to an increase in the RM size. The above discussion can explain why at low W_0, benzene/G12-2-12/*n*-octanol/water RMs are larger than those of DTAB in the same experimental conditions.

A different scenario is presented for benzene/G12-2-12/*n*-pentanol/water RMs. When the amount of water increases, there is an initial linear growth of the droplet sizes and, the d_{app} value increases from 6.1 nm at W_0 = 5 to 8.7 nm at W_0 = 8. After that, no change in the diameter is observed, and the d_{app} values remain constant at around 9 nm.

It is well-known that the increment in the RMs droplet size values is attributed to interaction between the polar solvent entrapped and the RM interface.[49] However, the absence of variation in the droplets sizes can be due to different reasons: (i) the first explanation that comes out is that the polar solvent molecules are not dispersed and are dissolved in the external pseudophase (if it is possible). (ii) Another possibility is that polar solvent molecules are encapsulated by the surfactant but do not interact with the interface. In other words, the polar solvent creates a true polar pool without interacting with the surfactant. Both hypotheses give d_{app} values that do not change with the polar solvent content.[39] In our case, the first possibility is discarded due to the known insolubility of water in the external solvent. In the FTIR section, we will demonstrate the weaker water−surfactant interaction when *n*-pentanol is used as cosurfactant.

3.4. RMs Interfacial Composition. In order to explore the relation between the micellar size and the interfacial composition, SLS measurements were performed, and M_w values were obtained for W_0 = 5 and W_0 = 10. Using the dilution method (see Experimental Section), the molar fraction of *n*-alcohol in the interface (X^i_a) and thus the interfacial composition of the gemini RMs was obtained for different values of W_0 (Figures S1 and S2 in Supporting Information). This information was introduced in eq 12 to obtain the number of surfactants at the micellar interface and thus the micellar aggregation number, N_{agg}. All data obtained are summarized in Table 2, and it is important to highlight the following: (a) *n*-Alcohol distribution constant (K_d) decreases with W_0 showing a change in slope at W_0 = 10, indicating that below this value of W_0, G12-2-12 polar heads are involved in the hydration process, whereas at higher W_0, the water forms a polar pool; (b) The aggregation number at W_0 = 5 is similar for the systems containing *n*-pentanol and *n*-octanol; however at W_0 = 10, the system containing *n*-pentanol has more molecules of surfactant per micelle than the *n*-octanol one; (c) *n*-Alcohol molar fraction at the interface (X^i_a) decreases increasing W_0 values, indicating that *n*-alcohol molecules are expelled into the nonpolar external phase as the water content inside the RMs increases. For *n*-pentanol the decreases in X^i_a is until W_0 = 10, and after that, they remain constant. For *n*-octanol, X^i_a values decrease in the whole W_0 range investigated. One way to explain these results is to consider that *n*-pentanol and *n*-octanol are located in slightly different regions in the RM interface: *n*-octanol (long hydrocarbon chain) locates at the RMs interface among the surfactant hydrocarbon tails, increasing the water−surfactant polar headgroup interaction as Scheme 2A shows. This explains the linear decreases in the X^i_a value of *n*-octanol increasing the water content. On the other hand, the short hydrocarbon chain of *n*-pentanol allows the alcohol to locate itself at the RMs interface near the polar core (see Scheme 2B), limiting the interaction of water with the micellar inner interface. This location probably prevents the decreases of X^i_a value of the *n*-pentanol with W_0. To probe this hypothesis, it is important to explore the behavior of the water

Table 2. K_d, X^i_a, M_w, n^i_s, in Function of the W_0 for G12-2-12 Surfactant in Benzene with *n*-Pentanol and *n*-Octanol as Cosurfactant

	n-pentanol				*n*-octanol			
W_0	K_d	X^i_a	M_w	n^i_s	K_d	X^i_a	M_w	n^i_s
5	37.0	0.713	10764	11.7	68.5	0.779	10060	9.9
7.5	26.5	0.700			35.1	0.762		
10	19.7	0.661	41493	42.9	24.9	0.743	36630	34.9
15	18.4	0.660			22.6	0.688		
20	21.9	0.661			22.0	0.636		

DOI: 10.1021/acs.jpcb.5b10380
J. Phys. Chem. B 2016, 120, 467−476

Scheme 2. Schematic Representation of Gemini RM Interface in the Presence of *n*-Octanol (A) and *n*-Pentanol (B) as Cosurfactant

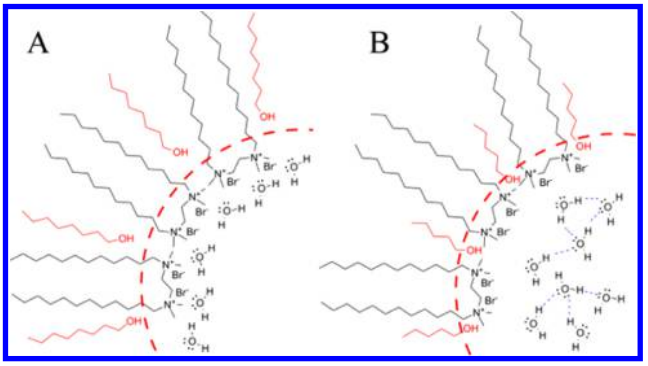

molecules inside the RMs and gain insight of the processes that occurs in the formation of gemini RMs.

3.5. Water Structure Studied by FT-IR. In order to get insights about the water structure dispersed by the gemini RMs, we carried out several FT-IR studies. Thus, we focus on the O−D stretching mode of the entrapped water molecules.

It is well-known that water and alcohols molecules exhibit a broad band in the 3500−3200 cm^{-1} region, which is assigned to the O−H stretching.[50] In liquid phase, this band not only corresponds to the O−H stretching but also to the vibrational coupling of the H−O−H bonds.[51,52] This phenomenon is also observed for deuterated water (D_2O) in which the band recorded in the 2570−2350 cm^{-1} region, also broad, corresponds to the O−D stretching mode and the vibrational couplings of the D−O−D bonds. In RMs, the most common method to obtain information is the curve fitting of the different IR peaks, e.g., ν_{O-H} of entrapped water or ν_{O-D} of entrapped D_2O.[28,53−55] However, the basic premise involved in this assumption, i.e., that each band obtained by curve fitting may be attributed to a different type of water, is open to question because these bands possibly originate from coupled water molecule vibrations, and from a bending overtone often reported in the spectrum of liquid water.[56] Consequently, in our FT-IR studies, we decided to use monodeuterated water (HDO), which exhibits a narrow band around 2570−2350 cm^{-1} that can be assigned only to the O−D stretching band (ν_{O-D}) since it is not coupled to any vibration mode.[49,53,55] This methodology was used before in other aqueous RMs in order to avoid the vibrational coupling and simplify the data analysis[57] and is very useful considering the highly complex 3500−3200 cm^{-1} region in the present system (see discussion in Supporting Information of Figures S5 and S6 for a detailed analysis of the 3500−3200 cm^{-1} region).

3.5.1. Homogeneous Medium. For a right interpretation of the results in the micellar medium, it is important to characterize what happens in the solvent used to prepare the RMs (i.e., benzene). Moreover, it is interesting to monitor the water behavior dissolved as trace in benzene to understand its spectra when it is not dissolved in a confined environment. Benzene saturated with monodeuterated water shows a small peak located at 2674 cm^{-1} (Figure S3) while the *n*-pentanol/benzene and *n*-octanol/benzene systems saturated with water show the same peak at 2664 cm^{-1} with an extra band with very small absorbance located around 2470 cm^{-1} (data not shown). This fact probably indicates the presence of isolated water molecules dissolved in the nonpolar solvent, as monomer, which provide an observable signal. Thus, these bands have to be taken into consideration when analyzing the RMs media. On the other hand, pure monodeuterated water shows a board symmetric band that peaks at 2515 cm^{-1} which is best fitted with a Gaussian function.[58]

3.5.2. RMs Media. 3.5.2.1. Variation of Gemini and DTAB Concentration. FTIR spectra of G12-2-12 RM system increasing the surfactant concentration with constant *n*-pentanol content and W_0 value are presented in Figure 2

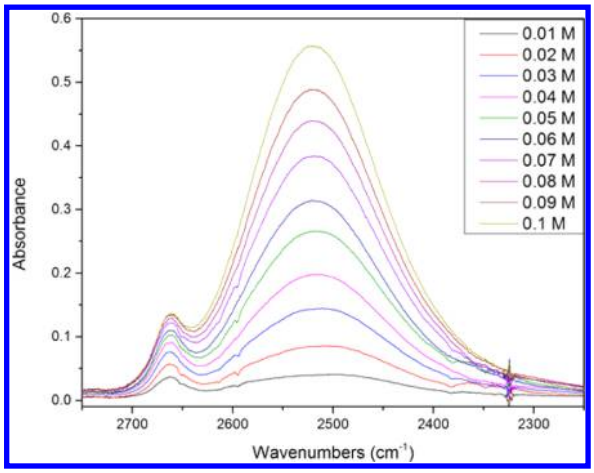

Figure 2. FTIR spectra of water inside G12-2-12/*n*-pentanol/benzene RMs varying G12-2-12 concentration at W_0 = 10 and [*n*-pentanol] = 0.7 M in the region 2300−2800 cm^{-1} (υ_{OD}).

(water/G12-2-12/*n*-octanol/benzene system in Figure S4 in Supporting Information). Two peaks were found in the OD region for both systems: a small peak located at 2664 cm^{-1} and the other located around 2520 cm^{-1}. Each spectrum was deconvoluted using Voigt function revealing that both peaks have a Gaussian distribution (>99%). Figure 3 shows the areas of each peak for the systems water/G12-2-12/*n*-pentanol/benzene and water/G12-2-12/*n*-octanol/benzene both at W_0 = 10 plotted against G12-2-12 concentration. While the peak located at 2664 cm^{-1} shows no increment of its area with the total amount of water in the system and no shift on its

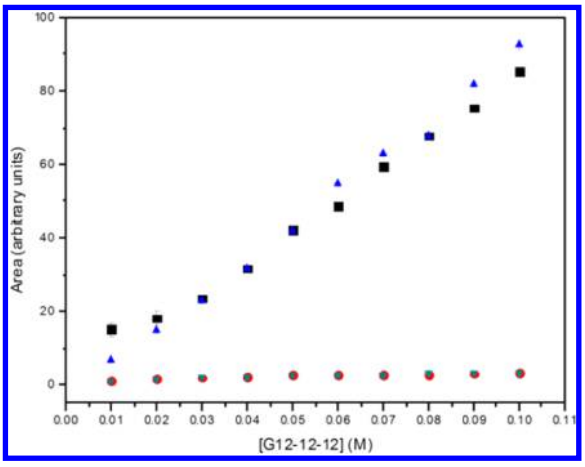

Figure 3. Area of the peaks υ_{OD} of water in the Gemini RM varying G12-2-12 concentration at W_0 = 10. Water inside RM = (■) 2550 cm^{-1}, *n*-pentanol; (blue ▲) 2550 cm^{-1}/ *n*- *n*-octanol; Water outside RM = (green ▼) 2663 cm^{-1}/ *n*-octanol; (red ●) 2663 cm^{-1}, *n*-pentanol.

DOI: 10.1021/acs.jpcb.5b10380
J. Phys. Chem. B 2016, 120, 467−476

maximum with the surfactant concentration, the peak located at 2520 cm^{-1} exhibits linear increases of its area with the amount of water in the system for both cosurfactants used. These results suggest that the first band can be assigned to water solubilizated in the external medium, and the latter corresponds to the water encapsulated inside the RM. Interestingly, the band around 2500 cm^{-1} displays two different behaviors when *n*-pentanol and *n*-octanol are used as cosurfactant, as shown in Figure 4. When *n*-pentanol is used, the shift of the maximum of

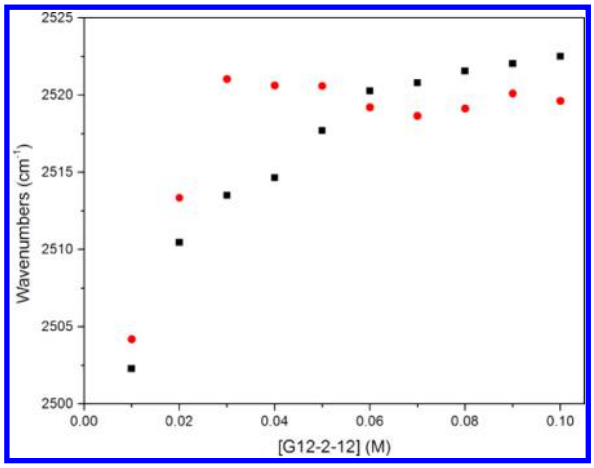

Figure 4. Maximum of the peak υ_{OD} of water inside RM varying G12-2-12 concentration at W_0 = 10 and [*n*-alcohol] = 0.7 M. (■) Gemini/*n*-pentanol, (red ●) Gemini/*n*-octanol.

the peak occurs smoothly going from 2502 to 2522 cm^{-1}, increasing the G12-2-12 concentration from 0.01 to 0.1 M. On the other hand, for *n*-octanol the shift occurs from 0.01 to 0.03 M going from 2504 to 2520 cm^{-1}, and after that, no changes in the maximum is observed with the surfactant concentration.

3.5.2.2. Variation of W_0. FTIR spectra of water inside G12-2-12/*n*-pentanol/benzene RMs varying W_0 while leaving surfactant concentration constant are shown in Figure 5. This experiment was carried out for the gemini and DTAB surfactants both using *n*-pentanol and *n*-octanol as cosurfactants (see Supporting Information Figures S7, S8, and S9 for G12-2-12/*n*-octanol/benzene, DTAB/*n*-pentanol/benzene and

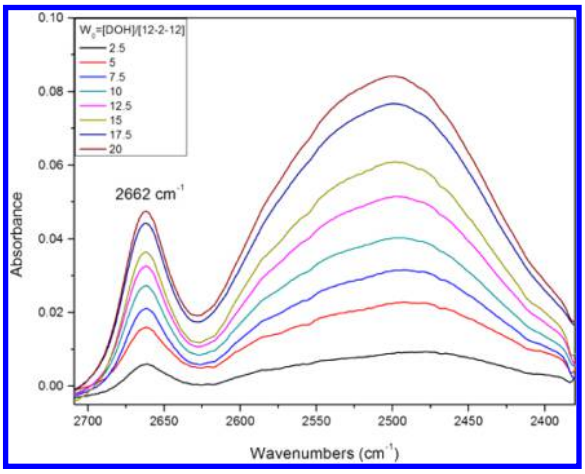

Figure 5. FTIR spectra of water inside G12-2-12/*n*-pentanol/benzene RMs varying W_0 at [G12-2-12] = 0.01 M and [*n*-pentanol] = 0.7 M in the region 2300−2800 cm^{-1} (υ_{OD}).

DTAB/*n*-octanol/benzene systems, respectively). In all systems, the variation of the water content at constant concentration of surfactant produces an increases in the absorbance of the peak located near 2500 cm^{-1}, indicating that water is being encapsulated inside the RMs. The shift of the maximum of the band corresponding to the water inside the RMs for each of these systems is plotted in Figure 6. Water

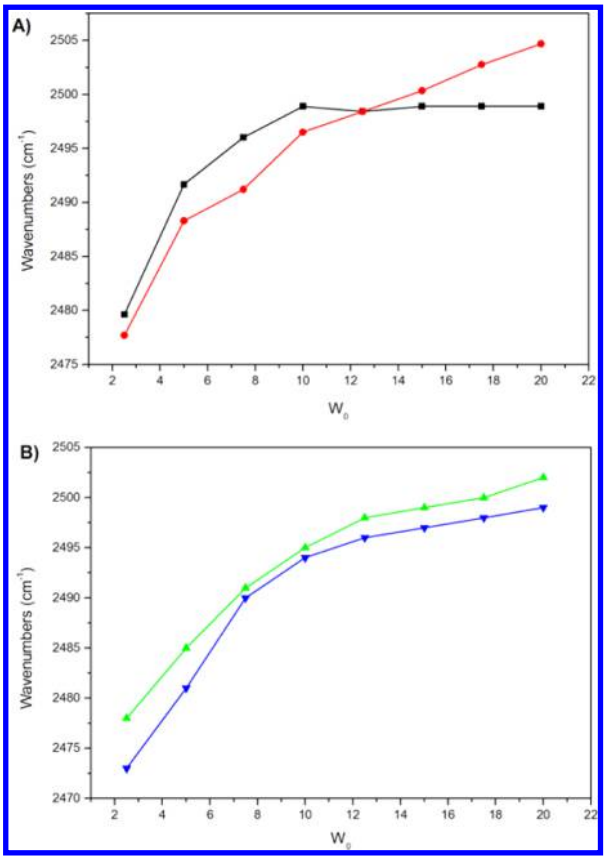

Figure 6. Maximum of the peak υ_{OD} of water inside RM varying W_0 at surfactant concentration fixed at 0.01 M and [*n*-alcohol] = 0.7 M constant. A) (■) G12-2-12/ *n*-pentanol, (red ●) G12-2-12/ *n*-octanol, B) (green ▲) DTAB/*n*-pentanol and (blue ▼) DTAB/*n*-octanol. Bulk water υ_{OD} frequency = 2515 cm^{-1}.

entrapped in all cationic RMs appears at lower frequencies than neat water. This fact can be explained by considering that in cationic RMs the cationic polar headgroup is solvated by ion−dipole interactions through the nonbonding electrons pairs of oxygen, which leads to a smaller force constant in the O−H bond.[50] All systems reveal a shift to higher frequencies with the increase of W_0, indicating that water inside the RMs tends to behave more as bulk water as the amount of water increases, increasing the hydrogen bond frequency. Around W_0 = 10, both DTAB RMs show a change in the slope presumably, indicating that up to W_0 = 10, the RM interface has been hydrated by water molecules and after that point added water still interacts with the interface but is forming a bulk like polar core. For the G12-2-12/*n*-octanol system, the behavior is similar to the one for DTAB/*n*-octanol but with higher frequency showing the same breaking point at W_0 = 10. On the other hand, G12-2-12/*n*-pentanol exhibits an interesting behavior: water added below W_0 = 10 produces a shift in the maximum of the peak located around 2500 cm^{-1}, but after that, there is no further shift on the peak. Thus, for W_0 < 10, the interface has been hydrated by

DOI: 10.1021/acs.jpcb.5b10380
J. Phys. Chem. B 2016, 120, 467−476

both the alcohol and the water, and all extra water added at $W_0 > 10$ forms a water pool that does not interact with the micellar. Knowing that the increase of RMs droplet sizes is mainly affected by the interaction of the polar solvent with the RMs interface, a system where the solvent entrapped do not interact with the RMs interface should not show variation with W_0. For the G12-2-12/*n*-pentanol RMs system, we found the same result using DLS and FTIR experiments. Thus, the growth of the RMs is fully controlled by the interaction of water with the RMs interface, which depends dramatically on the length of the hydrocarbon chain of the cosurfactant used.

4. CONCLUSION

For the first time, the droplet sizes of the RMs created using G12-2-12 as surfactant and two different alcohols as cosurfactants were determined by DLS, and the water structure and water−surfactant interaction were investigated using FT-IR. The results reveal that the structure of the cosurfactant needed to stabilize the RMs plays a fundamental role, affecting the size and the interfacial composition of the RMs. Thus, *n*-pentanol and *n*-octanol are located in different regions in the RM interface. *n*-Octanol locates at the RMs interface among the surfactant hydrocarbon tails, increasing the water−surfactant polar headgroup interaction. On the other hand, *n*-pentanol locates at the RMs interface near the polar core, limiting the interaction of water with the micellar inner interface and favoring the water−water interaction in the polar core. In comparison with the monomeric surfactant, DTAB presents no sensitivity to the kind of alcohols used as cosurfacant, and water always interacts with the polar head.

All these results indicate that gemini RMs are particularly sensitive to small changes in the condition of the experiment. These properties render numerous ways to control the size, concentration, and interfacial composition. This behavior may become very important when these systems are used as nanoreactors and in particular for nanoparticles synthesis.

■ ASSOCIATED CONTENT

Supporting Information

The Supporting Information is available free of charge on the ACS Publications website at DOI: 10.1021/acs.jpcb.5b10380.

(1) Details of the synthesis and characterization of G12-2-12 surfactant. (2) Discussion on the homogeneous mixtures of *n*-pentanol:benzene. (3) Apparent micellar diameter obtained with DLS and the corresponding polydispersity index (Table S1). (4) The n_a/n_s vs n_o/n_s plots for water/G12-2-12/*n*-alcohol/benzene (Figures S1 and S2). (5) FTIR spectra of benzene saturated with monodeuterated water (Figure S3). (6) FTIR spectra of water inside G12-2-12/*n*-octanol/benzene micelles (Figure S4). (7) FTIR spectra of *n*-alcohol/benzene blends (Figures S5 and S6). (8) FTIR spectra of water inside surfactant/*n*-alcohol/benzene RMs varying W_0 (Figures S7, S8, and S9) (PDF)

■ AUTHOR INFORMATION

Corresponding Author

*E-mail: mcorrea@exa.unrc.edu.ar.

Notes

The authors declare no competing financial interest.

■ ACKNOWLEDGMENTS

We gratefully acknowledge the financial support for this work by the Consejo Nacional de Investigaciones Científicas y Técnicas (CONICET), Agencia Nacional de Promoción Científica y Técnica and Secretaría de Ciencia y Técnica de la Universidad Nacional de Río Cuarto. N.M.C., J.J.S. and R.D.F. hold a research position at CONICET. V.E.C. thanks CONICET for a research fellowship.

■ REFERENCES

(1) Correa, N. M.; Silber, J. J.; Riter, R. E.; Levinger, N. E. Nonaqueous Polar Solvents in Reverse Micelle Systems. *Chem. Rev.* **2012**, *112*, 4569−4602.

(2) De, T. K.; Maitra, A. Solution Behaviour of Aerosol OT in Non-Polar Solvents. *Adv. Colloid Interface Sci.* **1995**, *59*, 95−193.

(3) Mandal, D.; Ghosh, M.; Maiti, S.; Das, K.; Das, P. K. Water-in-Oil Microemulsion Doped with Gold Nanoparticle Decorated Single Walled Carbon Nanotube: Scaffold for Enhancing Lipase Activity. *Colloids Surf., B* **2014**, *113*, 442−449.

(4) Zhang, D.; Liu, X.; Wang, X.; Yang, X.; Lu, L. Optical Properties of Monodispersed Silver Nanoparticles Produced Via Reverse Micelle Microemulsion. *Phys. B* **2011**, *406*, 1389−1394.

(5) Moyano, F.; Falcone, R. D.; Mejuto, J. C.; Silber, J. J.; Correa, N. M. Cationic Reverse Micelles Create Water with Super Hydrogen-Bond-Donor Capacity for Enzymatic Catalysis: Hydrolysis of 2-Naphthyl Acetate by α-Chymotrypsin. *Chem. - Eur. J.* **2010**, *16*, 8887−8893.

(6) Silva, O. F.; Fernández, M. A.; Silber, J. J.; de Rossi, R. H.; Correa, N. M. Inhibited Phenol Ionization in Reverse Micelles: Confinement Effect at the Nanometer Scale. *ChemPhysChem* **2012**, *13*, 124−130.

(7) Lopez, F.; Cinelli, G.; Ambrosone, L.; Colafemmina, G.; Ceglie, A.; Palazzo, G. Role of the Cosurfactant in Water-in-Oil Microemulsion: Interfacial Properties Tune the Enzymatic Activity of Lipase. *Colloids Surf., A* **2004**, *237*, 49−59.

(8) Giustini, M.; Palazzo, G.; Colafemmina, G.; Della Monica, M.; Giomini, M.; Ceglie, A. Microstructure and Dynamics of the Water-in-Oil CTAB/n-Pentanol/n-Hexane/Water Microemulsion: A Spectroscopic and Conductivity Study. *J. Phys. Chem.* **1996**, *100*, 3190−3198.

(9) Atik, S. S.; Thomas, J. K. Abnormally High Ion Exchange in Pentanol Microemulsions Compared to Hexanol Microemulsions. *J. Phys. Chem.* **1981**, *85*, 3921−3924.

(10) Mathew, D. S.; Juang, R.-S. Role of Alcohols in the Formation of Inverse Microemulsions and Back Extraction of Proteins/Enzymes in a Reverse Micellar System. *Sep. Purif. Technol.* **2007**, *53*, 199−215.

(11) Graciaa, A.; Lachaise, J.; Cucuphat, C.; Bourrel, M.; Salager, J. L. Improving Solubilization in Microemulsions with Additives. 1. The Lipophilic Linker Role. *Langmuir* **1993**, *9*, 669−672.

(12) Graciaa, A.; Lachaise, J.; Cucuphat, C.; Bourrel, M.; Salager, J. L. Improving Solubilization in Microemulsions with Additives. 2. Long Chain Alcohols as Lipophilic Linkers. *Langmuir* **1993**, *9*, 3371−3374.

(13) Salager, J. L.; Graciaa, A.; Lachaise, J. Improving Solubilization in Microemulsions with Additives. Part III: Lipophilic Linker Optimization. *J. Surfactants Deterg.* **1998**, *1*, 403−406.

(14) Abuin, E.; Lissi, E.; Olivares, K. Tetradecyltrimethylammonium Bromide Water-in-Oil Microemulsions: Dependence of the Minimum Amount of Alkanol Required to Produce a Microemulsion with the Alkanol and Organic Solvent Topology. *J. Colloid Interface Sci.* **2004**, *276*, 208−211.

(15) Agazzi, F. M.; Rodriguez, J.; Falcone, R. D.; Silber, J. J.; Correa, N. M. PRODAN Dual Emission Feature To Monitor BHDC Interfacial Properties Changes with the External Organic Solvent Composition. *Langmuir* **2013**, *29*, 3556−3566.

(16) Ranjan, R.; Vaidya, S.; Thaplyal, P.; Qamar, M.; Ahmed, J.; Ganguli, A. K. Controlling the Size, Morphology, and Aspect Ratio of Nanostructures Using Reverse Micelles: A Case Study of Copper Oxalate Monohydrate. *Langmuir* **2009**, *25*, 6469−6475.

DOI: 10.1021/acs.jpcb.5b10380
J. Phys. Chem. B 2016, 120, 467−476

(17) Bumajdad, A.; Madkour, M.; Shaaban, E.; Seoud, O. A. E. FT-IR and 1H NMR Studies of the State of Solubilized Water in Water-in-oil Microemulsions Stabilized by Mixtures of Single- and Double-Tailed Cationic Surfactants. *J. Colloid Interface Sci.* **2013**, *393*, 210−218.
(18) Das, S.; Mukherjee, I.; Paul, B. K.; Ghosha, S. Physicochemical Behaviors of a Cationic Gemini Surfactant (14-4-14) Based Micro-Heterogeneous Assemblies. *Langmuir* **2014**, *30*, 12483−12493.
(19) Menger, F. M.; Keiper, J. S. Gemini Surfactants. *Angew. Chem., Int. Ed.* **2000**, *39*, 1906−1920.
(20) Zana, R. Dimeric and Oligomeric Surfactants. Behavior at Interfaces and in Aqueous Solution: A Review. *Adv. Colloid Interface Sci.* **2002**, *97*, 205−253.
(21) Acharya, D. P.; Gutiérrez, J. M.; Aramaki, K.; Aratani, K. I.; Kunieda, H. Interfacial Properties and Foam Stability Effect of Novel Gemini-Type Surfactants in Aqueous Solutions. *J. Colloid Interface Sci.* **2005**, *291*, 236−243.
(22) Cashion, M. P.; Li, X.; Geng, Y.; Hunley, M. T.; Long, T. E. Gemini Surfactant Electrospun Membranes. *Langmuir* **2010**, *26*, 678−683.
(23) Bernheim-Groswasser, A.; Zana, R.; Talmon, Y. Sphere-to-Cylinder Transition in Aqueous Micellar Solution of a Dimeric (Gemini) Surfactant. *J. Phys. Chem. B* **2000**, *104*, 4005−4009.
(24) Wu, D.; Feng, Y.; Xu, G.; Chen, Y.; Cao, X.; Li, Y. Dilational Rheological Properties of Gemini Surfactant 1,2-Ethane Bis(Dimethyl Dodecyl Ammonium Bromide) at Air/Water Interface. *Colloids Surf., A* **2007**, *299*, 117−123.
(25) Zheng, O.; Zhao, J.-X.; Fu, X.-M. Interfacial Composition and Structural Parameters of Water/C12-*s*-C12·2Br/*n*-Hexanol/*n*-Heptane Microemulsions Studied by the Dilution Method. *Langmuir* **2006**, *22*, 3528−3532.
(26) Zheng, O.; Zhao, J. X.; Chen, R. T.; Fu, X. M. Aggregation of Quaternary Ammonium Gemini Surfactants C12-*s*-C12·2Br in *n*-Heptane/*n*-Hexanol Solution: Effect of the Spacer Chains on the Critical Reverse Micelle Concentrations. *J. Colloid Interface Sci.* **2006**, *300*, 310−313.
(27) Zhao, J. X.; Deng, S. J.; Liu, J. Y.; Lin, C. Y.; Zheng, O. Fourier Transform Infrared Investigation on the State of Water in Reverse Micelles of Quaternary Ammonium Gemini Surfactants C12-s-C(12).2Br in n-heptane. *J. Colloid Interface Sci.* **2007**, *311*, 237−242.
(28) Novaki, L. P.; Seoud, O. A. E. A Fourier Transform Infrared Study on the Structure of Water Solubilized by Reverse Aggregates of Sodium and Magnesium bis(2-Ethylhexyl) Sulfosuccinates in Organic Solvents. *J. Colloid Interface Sci.* **1998**, *202*, 391−398.
(29) Mundy, W. C.; Gutierrez, L.; Spedding, F. H. Raman Intensities of the Uncoupled OD Oscillators in Liquid Water. *J. Chem. Phys.* **1973**, *59*, 2173−2182.
(30) Wiafe-Akenten, J.; Bansil, R. Intermolecular Coupling in HOD Solutions. *J. Chem. Phys.* **1982**, *78*, 7132−7137.
(31) Mikenda, W. IR Study of Cation Effects on the O-D Stretching Frequencies of Isotopically Dilute HDO in Aqueous Salt Solutions. *Monatsh. Chem.* **1986**, *117*, 977−984.
(32) Lindgren, J.; Hermansson, K.; Wójcik, M. J. Theoretical Simulation and Experimental Determination of OH and OD Stretching Bands of Isotopically Diluted HDO Molecules in Aqueous Electrolyte Solutions. *J. Phys. Chem.* **1993**, *97*, 5254−5259.
(33) Lide, D. R. *CRC Handbook of Chemistry and Physics*, 84th ed.; CRC Press: Boca Raton, FL, 2003.
(34) Gracia, C. A.; Gómez-Barreiro, S.; González-Pérez, A.; Nimo, J.; Rodríguez, J. R. Static and Dynamic Light-scattering Studies on Micellar Solutions of Alkyldimethylbenzylammonium Chlorides. *J. Colloid Interface Sci.* **2004**, *276*, 408−413.
(35) Bender, T. M.; Lewis, R. J.; Pecora, R. Absolute Rayleigh Ratios of Four Solvents at 488 nm. *Macromolecules* **1986**, *19*, 244−245.
(36) Birdi, K. S. Microemulsions: Effect of Alkyl Chain Length of Alcohol and Alkane. *Colloid Polym. Sci.* **1982**, *260*, 628−631.
(37) Singh, H. N.; Swarup, S.; Singh, R. P.; Saleem, S. M. Structural Description of Water-in-Oil Microemulsions Using Electrical Resistance. *Ber. Bunsen-Ges.* **1983**, *87*, 1115−1120.
(38) Moulik, S. P.; Digout, L. G.; Aylward, W. M.; Palepu, R. Studies on the Interfacial Composition and Thermodynamic Properties of W/O Microemulsions. *Langmuir* **2000**, *16*, 3101−3106.
(39) Durantini, A. M.; Falcone, R. D.; Silber, J. J.; Correa, N. M. More Evidence on the Control of Reverse Micelles Sizes. Combination of Different Techniques as a Powerful Tool to Monitor AOT Reversed Micelles Properties. *J. Phys. Chem. B* **2013**, *117*, 3818−3828.
(40) Riter, R. E.; Kimmel, J. R.; Undiks, E. P.; Levinger, N. E. Novel Reverse Micelles Partitioning Nonaqueous Polar Solvents in a Hydrocarbon Continuous Phase. *J. Phys. Chem. B* **1997**, *101*, 8292−8297.
(41) Berne, B. J.; Pecora, R. *Dynamic Light Scattering: With Applications to Chemistry, Biology, and Physics*; John Wiley & Sons, Inc.: New York, 1976.
(42) Blach, D.; Silber, J. J.; Correa, N. M.; Falcone, R. D. Electron Donor Ionic Liquids Entrapped in Anionic and Cationic Reverse Micelles. Effects of the Interface on the Ionic Liquid-Surfactant Interactions. *Phys. Chem. Chem. Phys.* **2013**, *15*, 16746−16757.
(43) Ferreyra, D. D.; Correa, N. M.; Silber, J. J.; Falcone, R. D. The Effect of Different Interfaces and Confinement on the Structure of the Ionic Liquid 1-Butyl-3-Methylimidazolium Bis-(Trifluoromethylsulfonyl)imide Entrapped in Cationic And Anionic Reverse Micelles. *Phys. Chem. Chem. Phys.* **2012**, *14*, 3460−3470.
(44) Salabat, A.; Eastoe, J.; Mutch, K. J.; Tabor, R. F. Tuning Aggregation of Microemulsion Droplets and Silica Nanoparticles Using Solvent Mixtures. *J. Colloid Interface Sci.* **2008**, *318*, 244−251.
(45) Maitra, A. Determination of Size Parameters of Water-Aerosol OT-Oil Reverse Micelles From Their Nuclear Magnetic Resonance Data. *J. Phys. Chem.* **1984**, *88*, 5122−5125.
(46) Tanford, C. Micelle Shape and Size. *J. Phys. Chem.* **1972**, *76*, 3020−3024.
(47) Danino, D.; Talmon, Y.; Zana, R. Alkanediyl-α,ω-Bis-(Dimethylalkylammonium Bromide) Surfactants (Dimeric Surfactants). 5. Aggregation and Microstructure in Aqueous Solutions. *Langmuir* **1995**, *11*, 1448−1456.
(48) Almeida, J. A. S.; Pinto, S. P. R.; Wang, Y.; Marques, E. F.; Pais, A. A. C. C. Structure and Order of DODAB Bilayers Modulated by Dicationic Gemini Surfactants. *Phys. Chem. Chem. Phys.* **2011**, *13*, 13772−13782.
(49) Falcone, R. D.; Silber, J. J.; Correa, N. M. What are the Factors that Control Non-Aqueous/AOT/n-Heptane Reverse Micelle Sizes? A Dynamic Light Scattering Study. *Phys. Chem. Chem. Phys.* **2009**, *11*, 11096−11100.
(50) Silverstein, R. M.; Webster, F. X.; Kiemle, D. J. *Spectrometric Identification of Organic Compounds*, 7th ed.; Wiley: New York, 2005.
(51) Pacynko, W. F.; Yarwood, J.; Tiddy, G. J. T. Infrared and Far-Infrared Spectroscopic Studies on the Structure of Water in Lyotropic Liquid Crystals. *Liq. Cryst.* **1987**, *2*, 201−214.
(52) Christopher, D. J.; Yarwood, J.; Belton, P. S.; Hills, B. P. A Fourier Transform Infrared Study of Water-Head Group Interactions in Reversed Micelles Containing Sodium Bis(2-Ethylhexyl) Sulfosuccinate (AOT). *J. Colloid Interface Sci.* **1992**, *152*, 465−472.
(53) Novaki, L. P.; Correa, N. M.; Silber, J. J.; El Seoud, O. A. FTIR and 1H NMR Studies of the Solubilization of Pure and Aqueous 1,2-Ethanediol in the Reverse Aggregates of Aerosol-OT. *Langmuir* **2000**, *16*, 5573−5578.
(54) Novaki, L. P.; Pires, P. A. R.; El Seoud, O. A. Fourier Transform-IR and 1H NMR Studies on the Structure of Water Solubilized by Reverse Aggregates of Calcium Bis(2-Ethylhexyl) Sulfosuccinate in Organic Solvents. *Colloid Polym. Sci.* **2000**, *278*, 143−149.
(55) El Seoud, O. A.; Correa, N. M.; Novaki, L. P. Solubilization of Pure and Aqueous 1,2,3-Propanetriol by Reverse Aggregates of Aerosol-OT in Isooctane Probed by FTIR and 1H NMR Spectroscopy. *Langmuir* **2001**, *17*, 1847−1852.
(56) Novaki, L. P.; El Seoud, O. A.; Lopes, J. C. D. An FT-IR Study on the Structure of Water Solubilized by Cetyltrimethylammonium Bromide Reverse Aggregates in Chloroform/n-Dodecane. *Ber. Bunsen-Ges.* **1997**, *101*, 1928−1932.

DOI: 10.1021/acs.jpcb.5b10380
J. Phys. Chem. B 2016, 120, 467−476

(57) Villa, C. C.; Silber, J. J.; Correa, N. M.; Falcone, R. D. Effect of the Cationic Surfactant Moiety on the Structure of Water Entrapped in Two Catanionic Reverse Micelles Created from Ionic Liquid-Like Surfactants. *ChemPhysChem* **2014**, *15*, 3097−3109.
(58) Falk, M. On the Satellite Bands Accompanying the OH and OD Stretching Fundamentals of Isotopically Dilute HDO in Ice Ih. *J. Chem. Phys.* **1987**, *87*, 28−30.

DOI: 10.1021/acs.jpcb.5b10380
J. Phys. Chem. B 2016, 120, 467−476